Hindawi Publishing Corporation
Dataset Papers in Science
Volume 2014, Article ID 684305, 13 pages
http://dx.doi.org/10.1155/2014/684305

Dataset Paper

ECLAT Cluster Spacecraft Magnetotail Plasma Region Identifications (2001–2009)

P. D. Boakes,[1] R. Nakamura,[1] M. Volwerk,[1] and S. E. Milan[2]

[1] *Space Research Institute, Austrian Academy of Sciences, 8042 Graz, Austria*
[2] *Department of Physics and Astronomy, University of Leicester, LE1 7RH Leicester, UK*

Correspondence should be addressed to P. D. Boakes; peter.boakes@oeaw.ac.at

Received 25 November 2013; Accepted 18 February 2014; Published 12 August 2014

Academic Editors: M. Iizima and K. Kudela

The European Space Agency's four-spacecraft Cluster mission has been observing the Earth's dynamical magnetotail region since early 2001. The magnetotail, and in particular the hot trapped plasma sheet, is a critical region in the coupled Sun-Earth system. Changes in the solar wind have direct influence on the properties and dynamical processes occurring in this region, which in turn directly influence operational near-Earth space, the upper atmosphere, and even induce large-scale currents in the ground. As part of the European Cluster Assimilation Technology (ECLAT) project, a magnetotail plasma region dataset has been produced to facilitate magnetospheric research and further our understanding of the important processes linking the solar wind-magnetospheric-ionospheric system. The dataset consists of a comprehensive list of plasma regions encountered in the nightside magnetosphere of the Earth by each of the four Cluster spacecraft in the years 2001–2009. The regions identified are those where major energy transport/conversion processes take place and are important regions for system level science. Characteristic averaged parameters describing the behavior of each region are provided for further understanding. The dataset facilitates the use of the large repository of Cluster data by the wider scientific community.

1. Introduction

The plasma environment of the Earth's magnetosphere (the region of near-Earth space governed by the Earth's magnetic field) provides an excellent natural laboratory to study fundamental plasma physics processes. Knowledge gained through the study of changes in this environment, and its dependence on Sun-Earth interactions, is important for satellite operation as well as understanding environmental and technological impacts on the surface of Earth (i.e., space weather). The fundamental interaction process resulting in the plasma environment at the Earth is the so-called Dungey cycle [1]. On the dayside of the Earth previously closed (with both footprints connected to the Earth) terrestrial magnetic field lines are split into two open magnetic field lines (with one footprint connected to the northern or southern hemisphere of the Earth, respectively, and the other connected to the solar wind) by magnetic reconnection. Solar wind particles can gain access to the Earth's magnetosphere through the high latitude open cusp regions. The opened magnetic field lines are swept by the solar wind flow to the nightside of the Earth, where they come together in the distant magnetotail and reconnect to form a newly closed magnetic field line which eventually circulates back around the flanks of the Earth to the dayside to complete the Dungey cycle. Solar wind particles slowly travel along open field lines in the tail region, forming the cold tenuous magnetospheric lobe regions at high latitudes. As the open lobe field lines are reconnected in the magnetotail by magnetic reconnection the solar wind particles are accelerated and heated to form a region of hot dense plasma trapped on closed magnetic field lines. This region is termed the plasma sheet and is often discussed in terms of a boundary region at the lobe-plasma sheet interface, which is expected to be directly connected to the magnetic reconnection region, and a central or inner plasma sheet region.

Several previous studies have made attempts to identify boundaries between different magnetotail plasma regions. Most of these studies use the bulk properties of the plasma, or instrument effects, to derive thresholds in the plasma beta (the ratio of the magnetic and plasma pressures) [2] and/or

plasma flow velocities [3, 4]. However, these studies and others [5, 6] have shown that defining plasma sheet regions by fixed threshold conditions is difficult, while Grigorenko et al. [7] suggest that on a case-to-case crossing of the plasma sheet the best way to determine the outer boundary of the plasma sheet is through manual inspection of full 3D plasma velocity distributions. The work of Grigorenko and Koleva [8] further showed the complicated nature of defining the outer regions of the plasma sheet by defining three different states based on the presence and characteristics of ion and electron beams at the lobe-plasma sheet interface.

Several dynamical processes occur in the plasma sheet region, causing space weather effects from space to the ground, the visible manifestation of which is the aurora. Such processes involve coupling among different regions and require in situ observation to be understood. Since 2001, the European Space Agency's four-spacecraft Cluster mission [9] has been observing these processes at an unprecedented level of detail. However, the wealth of information provided by the 11 instruments onboard of each Cluster spacecraft is hard to analyze without contextual knowledge of the plasma region being identified beforehand. The primary purpose of this dataset is to facilitate coordinated analysis of the magnetosphere at a system level, for example, providing a convenient and effective means for non-Cluster experts (e.g., ionospheric scientists) to understand the processes occurring in the magnetotail in relation to observations made by other observatories (i.e., ground-based and/or other spacecraft). The dataset also provides to Cluster scientists a quick and convenient means to determine the Cluster plasma region and environment, facilitating the selection of interesting periods for detailed or statistical analysis.

Taking advantage of the unique 4-spacecraft configuration of the Cluster mission, a new method has been achieved in deriving thresholds in plasma beta and magnetic field parameters to identify different plasma regions in the Earth's magnetotail region for 9 years of Cluster data (2001–2009). In order to provide as much contextual information as possible, a variety of averaged region parameters describing each region are given, along with caveats and data flags. A description of both these parameters and flags is given in the following sections. It is strongly recommended that the users of the database take note of, and consider, the effect of caveats and region parameters when analyzing the region data. For example, statistically unusual regions are flagged, for example, the cold dense plasma inside the inner plasma sheet region [10].

The database was created as part of the European Union Framework 7 Programme Project ECLAT, whose aim is to provide contextual data for the Cluster mission (http://www.eclat-project.eu/). This contextual data will all be made available through the existing repository of Cluster data, the Cluster Active Archive ([11] http://cosmos.esa.int/web/csa).

2. Methodology

The Cluster mission is a four-spacecraft mission launched in the summer of 2000 (data provided from early 2001) to investigate the three-dimensional structure in key plasma regions of the Earth's magnetosphere. The four identical spacecraft are flown in a constellation configuration with initial perigee of $4R_E$ (26,000 km), apogee of $19.6R_E$ (125,000 km or 19.6 Earth radii), and a tetrahedron separation of ~200–10,000 km in the magnetotail region. The Cluster mission is designed to observe a complete 360-degree sweep of the Earth's magnetosphere every year and therefore spends four months a year, July through October, in the target tail plasma regions of this dataset.

Each Cluster spacecraft (from here on referred to as C1, C2, C3, and C4) carries a suite of instruments to investigate electric and magnetic fields, as well as ion and electron distributions, of which the Fluxgate Magnetometer (FGM) [12], Cluster Ion Spectrometry experiment (CIS) [13], and The Plasma Electron and Current Experiment (PEACE) [14] are used in the identification of plasma regimes. FGM measures the magnetic field vectors, CIS measures the composition, mass, and distribution of ions in the energy range ~0–40 keV/q, and PEACE measures the electron distribution between 0.59 eV and 26.4 keV [11]. CIS consists of two separate instruments measuring the ion population, the Hot Ion Analyser (HIA), and the COmposition and DIstribution Function sensor (CODIF). While CODIF gives the mass per charge composition with medium angular resolution, allowing different ion species to be analyzed separately, HIA offers a better angular resolution but no mass separation of ion species. Of the CODIF ion species measured, measurements of H^+, the major ion population in the tail, only are used in the identification of different plasma regions and referred to in this report as CODIF-H1. In identifying tail plasma regions, we make use of CAA provided spin resolution (~4 second) moments data. This data consists of magnetic field and plasma moments (e.g., ion/electron density, temperature, velocity, and magnetic field components) averaged over 1 spacecraft spin from the full 3D particle distributions/high resolution magnetic field datasets [11]. Since magnetic field data from the FGM and plasma data from the CIS or PEACE are needed in region identification and the original dataset does not have the same time tags, the CAA FGM and plasma datasets are merged using the nearest neighbour's method. Separate merged datasets of FGM-HIA, FGM-CODIF H1, and FGM-PEACE data are created and used in the following analysis.

In order to identify the target plasma regions, extensive statistical studies of plasma and magnetic field moments for each tail season of the Cluster dataset (2001–2009) have been carried out, as well as analysis of individual plasma region crossings by the spacecraft. To avoid false identification of plasma sheet regions when the spacecraft enters other nontail plasma regions, such as the magnetosheath or inner magnetosphere regions, plasma regions are only identified within the tail region box $X < -8R_E$ and $|Y| < 15R_E$. GSM coordinates are used. Traditionally plasma beta (the ratio of plasma to magnetic field pressure) has been used to identify different plasma regions in the tail. We have taken advantage of the tetrahedron configuration of the four Cluster spacecraft to define different tail plasma regions and derive region thresholds in plasma beta and magnetic field based on the statistical profile of the tail current density. These current densities are derived from magnetic field gradients measured

between the four Cluster spacecraft, a well-known technique in space plasma physics termed the curlometer technique [15]. In short, FGM 5 HZ (200 ms) CAA provided datasets for each Cluster spacecraft are used to determine the net current through the spacecraft tetrahedron. An average of this data is then taken within 2 seconds of each data point in the merged FGM-plasma instrument datasets (resolution: 4 seconds) already created, such that the merged datasets also contain the current measurements at the same resolution of the moments data, from which the field-aligned and field-perpendicular components of the current can be determined.

Since the average plasma parameters in the tail remain relatively consistent throughout one yearly tail season, 4 months of data, region boundary conditions are determined for each of the tail seasons of the dataset (2001–2009) separately. The conditions are listed in Table 1. To illustrate how we define the tail plasma regions and determine the region boundary conditions, in Figures 1(a)–1(c) we show plasma density (a), the parallel component of the current density (b), and the perpendicular component of the current density (c) versus plasma beta for all measurements taken by all four Cluster spacecraft in the tail box region for the year 2002, using CODIF-H1 plasma measurements and GSM coordinates. The colour represents the number density, the red line represents the median, and the vertical lines represent the boundary locations. Histograms of the binned averages of these parameters, and the gradient of the median lines, are shown in Figures 2 and 3 at two scales to best visualise the different boundary locations. Figure 1(d) shows plasma beta (CODIF-H1) versus the magnitude of the xy component (i.e., $B_{xy} = \sqrt{B_x^2 + B_y^2}$) of the magnetic field as measured in GSM by the FGM instrument. The colour represents the plasma region. We define five plasma regions, where the hemisphere of the observing spacecraft is incorporated in the region name. Table 2 lists the regions identified in the dataset.

The first three plasma regions are defined using the current measurement (Figures 1(a)–1(c) and Figures 2 and 3) as follows.

(1) Lobe. The tail lobes are defined as the high latitude region of low plasma density and very soft ions/electrons corresponding to the region of open magnetic field lines. Only background currents are expected to be measured in this region and we define this region as the plasma beta region of background/noise level currents only (the lobe region is represented by the region left of the leftmost vertical dashed grey line in Figures 1(a)–1(c) and the grey region in Figure 1(d)).

(2) Boundary Region (BR). The transition region at the very edge of the plasma/current sheet; this is the plasma beta region where currents and plasma density are above the background level and increasing. The boundary is clearly marked by a decrease in the gradients of both current and plasma densities increase with beta (the BR is represented by the region bounded by the grey vertical dashed lines in Figures 1(a)–1(c) and the blue region of Figure 1(d). The lobe-BR boundary is seen in the top row of Figure 2 and the top two rows of Figure 3).

(3) Outer Plasma Sheet (OPS). The plasma beta region inside the BR transition region: the increase in density and currents with beta slows, with gradient lines decreasing. Perpendicular currents start to dominate over parallel currents, as expected inside the plasma sheet (the BR-OPS boundary is represented by the right hand vertical dashed grey line in Figures 1(a)–1(c), the bottom row of Figure 2, and the bottom two rows of Figure 3. The OPS region is represented by the orange region in Figure 1(d)).

All evidence from the statistical plots shown in Figures 1(a)–1(c) and Figures 2-3 is used to define the region thresholds. If the statistical boundary locations in currents and plasma density vary slightly, as may be expected due to the statistical nature of such analysis, we select the earliest boundary location or the most consistent boundary location between all three parameters. Separate analysis and plasma beta boundary identification is performed for each of the three plasma instruments (PEACE-electron plasma beta, HIA, and CODIF H1-ion plasma beta). Data from all available spacecraft are combined in the statistics from the relevant instruments, such that a boundary condition for any particular plasma instrument is consistent between spacecraft. While some plasma instruments failed to provide data from the start of the data provision period of the Cluster mission on one or more spacecraft, plasma instruments on other spacecraft also failed, or significantly degraded, at various epochs during the mission. While data from all working plasma instruments can be used when identifying target plasma regions, we select the instrument working to best quality for any given year and spacecraft to provide the final region boundaries. The plasma instrument used and boundary conditions for each year and spacecraft are shown in Table 1.

While the interface between the lobe and very edge of the plasma sheet can be a clear transition, the definition of the outer regions of the plasma sheet varies in the literature, as discussed in the introduction. The so-called Plasma Sheet Boundary Layer (PSBL) is often discussed as the very outer region of the plasma sheet, which is considered to be directly connected to the reconnection region. Many authors define this region as the region of high speed field-aligned velocity beams; however, other studies have shown these beams to be transient in nature and that they even can be classified into different types themselves [8]. Some studies assume a direct transition to the plasma sheet from the lobe (without a boundary layer region) if no high speed beams are observed, while other studies show that even in the absence of high speed beams there always exists a transition boundary region different from the more central plasma sheet [2]. In this dataset we follow the later convention, defining two outer regions (by the currents), with the percentage of high speed field parallel and field perpendicular velocity component provided as a parameter in each region record. The threshold of high speed is given by the three-sigma value of parallel and perpendicular flows recorded in all plasma sheet regions (BR, OPS, IPS, and NSR) for the relevant year

Table 1: Region identification, boundary conditions, and instruments used.

Region	SC	Instrument and condition								
		2001	2002	2003	2004	2005	2006	2007	2008	2009
LOBE	C1	CODIF H1 beta <0.02	CODIF H1 beta <0.025	CODIF H1 beta <0.015	HIA beta <0.009	HIA beta <0.01	HIA beta <0.01	HIA beta <0.022	HIA beta <0.02	HIA beta <0.025
	C2	PEACE beta <0.005	PEACE beta <0.008	PEACE beta <0.0025	PEACE beta <0.0055	PEACE beta <0.0055	PEACE beta <0.0065	PEACE beta <0.0065	PEACE beta <0.01	PEACE beta <0.013
	C3	CODIF H1 beta <0.02	CODIF H1 beta <0.025	HIA beta <0.009	HIA beta <0.009	HIA beta <0.01	HIA beta <0.01	HIA beta <0.022	HIA beta <0.02	HIA beta <0.025
	C4	CODIF H1 beta <0.02	CODIF H1 beta <0.025	CODIF H1 beta <0.015	CODIF H1 beta <0.015	CODIF H1 beta <0.01	CODIF H1 beta <0.017	CODIF H1 beta <0.017	CODIF H1 beta <0.015	CODIF H1 beta <0.02
BR	C1	CODIF H1 beta 0.02–0.12	CODIF H1 beta 0.025–0.16	CODIF H1 beta 0.015–0.12	HIA beta 0.009–0.07	HIA beta 0.01–0.08	HIA beta 0.01–0.08	HIA beta 0.022–0.09	HIA beta 0.02–0.1	HIA beta 0.025–0.16
	C2	PEACE beta 0.005–0.05	PEACE beta 0.008–0.05	PEACE beta 0.0025–0.03	PEACE beta 0.0055–0.025	PEACE beta 0.0055–0.06	PEACE beta 0.0065–0.02	PEACE beta 0.0065–0.056	PEACE beta 0.01–0.04	PEACE beta 0.013–0.035
	C3	CODIF H1 beta 0.02–0.12	CODIF H1 beta 0.025–0.16	HIA beta 0.009–0.05	HIA beta 0.009–0.07	HIA beta 0.01–0.08	HIA beta 0.01–0.08	HIA beta 0.022–0.09	HIA beta 0.02–0.1	HIA beta 0.025–0.16
	C4	CODIF H1 beta 0.02–0.12	CODIF H1 beta 0.025–0.16	CODIF H1 beta 0.015–0.12	CODIF H1 beta 0.015–0.16	CODIF H1 beta 0.01–0.17	CODIF H1 beta 0.017–0.08	CODIF H1 beta 0.017–0.13	CODIF H1 beta 0.015–0.3	CODIF H1 beta 0.02–0.13
OPS	C1	CODIF H1 beta >0.12 $B_{xy} > 13$	CODIF H1 beta >0.16 $B_{xy} > 15$	CODIF H1 beta >0.12 $B_{xy} > 14$	HIA beta >0.07 $B_{xy} > 14$	HIA beta >0.08 $B_{xy} > 15$	HIA beta >0.08 $B_{xy} > 15$	HIA beta >0.09 $B_{xy} > 13$	HIA beta >0.1 $B_{xy} > 13$	HIA beta >0.16 $B_{xy} > 11.5$
	C2	PEACE beta >0.05 $B_{xy} > 13$	PEACE beta >0.05 $B_{xy} > 15$	PEACE beta >0.0025 $B_{xy} > 14$	PEACE beta >0.0055 $B_{xy} > 14$	PEACE beta >0.0055 $B_{xy} > 15$	PEACE beta >0.0065 $B_{xy} > 15$	PEACE beta >0.0065 $B_{xy} > 13$	PEACE beta >0.01 $B_{xy} > 13$	PEACE beta >0.013 $B_{xy} > 11.5$
	C3	CODIF H1 beta >0.12 $B_{xy} > 13$	CODIF H1 beta >0.16 $B_{xy} > 15$	HIA beta >0.05 $B_{xy} > 14$	HIA beta >0.07 $B_{xy} > 14$	HIA beta >0.08 $B_{xy} > 15$	HIA beta >0.08 $B_{xy} > 15$	HIA beta >0.09 $B_{xy} > 13$	HIA beta >0.1 $B_{xy} > 13$	HIA beta >0.16 $B_{xy} > 11.5$
	C4	CODIF H1 beta >0.12 $B_{xy} > 13$	CODIF H1 beta >0.16 $B_{xy} > 15$	CODIF H1 beta >0.1 $B_{xy} > 14$	CODIF H1 beta >0.16 $B_{xy} > 14$	CODIF H1 beta >0.17 $B_{xy} > 15$	CODIF H1 beta >0.08 $B_{xy} > 15$	CODIF H1 beta >0.13 $B_{xy} > 13$	CODIF H1 beta >0.3 $B_{xy} > 13$	CODIF H1 beta >0.13 $B_{xy} > 11.5$
IPS	C1 C2 C3 C4	$B_{xy} < 13$	$B_{xy} < 15$	$B_{xy} < 14$	$B_{xy} < 14$	$B_{xy} < 15$	$B_{xy} < 15$	$B_{xy} < 13$	$B_{xy} < 13$	$B_{xy} < 11.5$
NSR	All SC	The region bracketing $B_x = 0$ crossing or $B_x = 0$ data point								

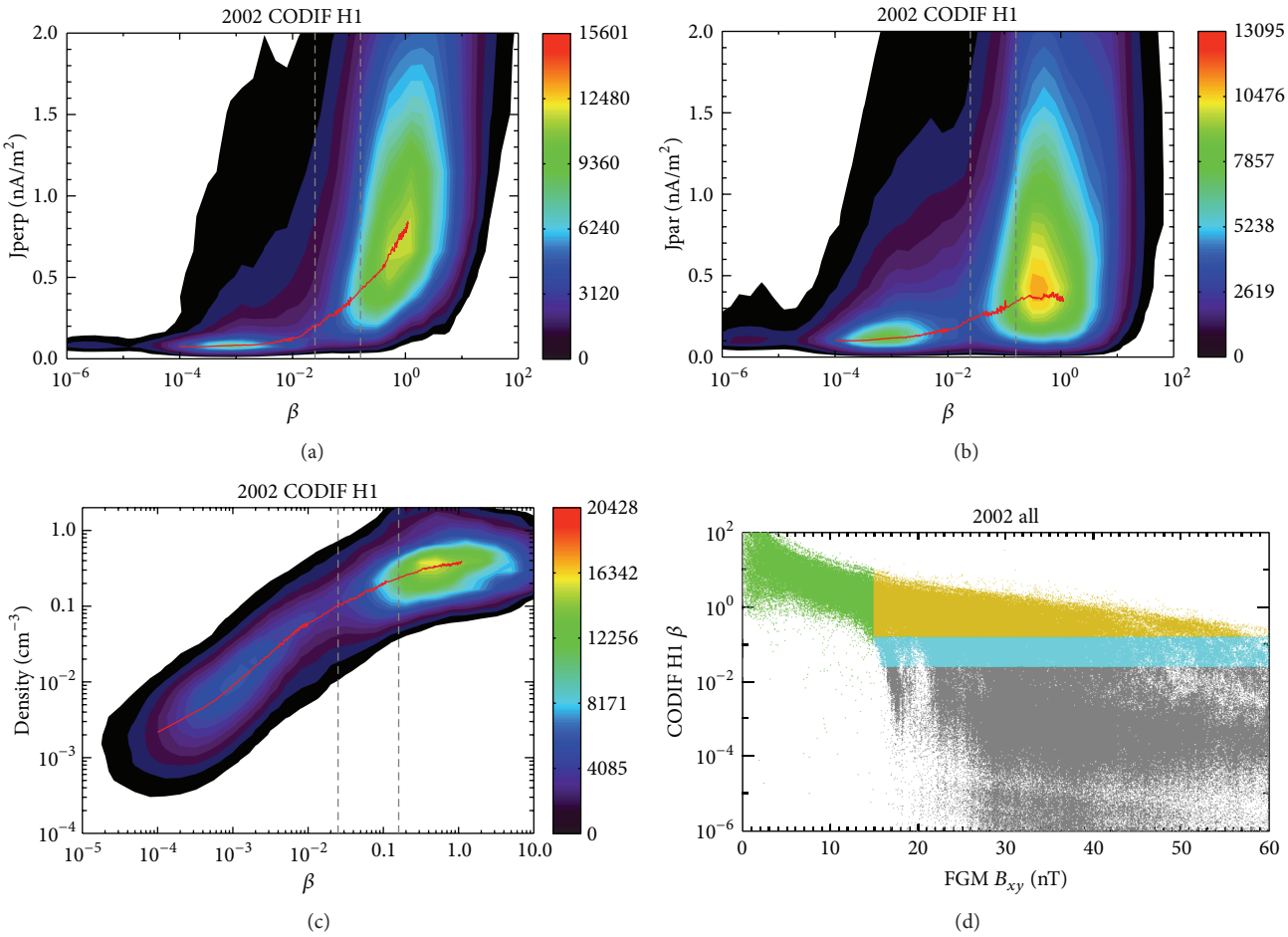

Figure 1: Example statistics of plasma and magnetic field moments used in determination of different plasma regions. Statistics are from all available Cluster moments in the tail season of 2002 (July–October) for the specified instrument and in the tail region X < $-8R_E$, |Y| < $15R_E$. ((a)–(c)) 2D histograms of currents perpendicular (Jperp, (a)) and parallel (Jpar, (b)) to the magnetic field, as well as plasma density (c), versus plasma beta. Colours represent the number of data points in each bin, and the red lines show the median. The left most dashed vertical lines show the statistical lobe-BR boundary condition, and the right hand dashed line represents the BR-OPS boundary condition. (d) Plasma beta versus magnetic field B_{xy} component. Different colours represent different plasma regions—grey: lobe, blue: BR, orange: OPS, and green: IPS.

Table 2: Region names.

Region name	Description
NN_LOBE	Northern hemisphere tail lobe region
SS_LOBE	Southern hemisphere tail lobe region
NN_BR	Northern hemisphere boundary region
SS_BR	Southern hemisphere boundary region
NN_OPS	Northern hemisphere outer plasma sheet
SS_OPS	Southern hemisphere outer plasma sheet
NN_IPS	Northern hemisphere inner plasma sheet
SS_IPS	Southern hemisphere inner plasma sheet
NS_NSR	North-south crossing of the neutral sheet
SN_NSR	South-north crossing of the neutral sheet
00_NSR	Neutral sheet data point, $B_x = 0$
UR	Undefined region

and plasma instrument. Values are listed in Table 3. Velocities are not provided when electron data from PEACE is used in the region determination (spacecraft C2), due to poor determination of electron velocity moments data by PEACE. While for the large majority of BR and OPS region intervals high speed field aligned beams are not observed, both BR and OPS regions can be "PSBL-like" with the presence of high speed beams recorded by the velocity parameters. Further, we define an inner plasma sheet (IPS) region where we expect no PSBL-like features to exist. The IPS is defined from, for example, Figure 1(d) as follows.

(4) Inner Plasma Sheet (IPS). It is the region adjacent to the neutral sheet and never directly connected to the lobe region. The boundary condition in B_{xy} is chosen by using similar figures as to Figure 1(d) to select the minimum B_{xy} value at the beta intersection between the OPS and BR regions. This procedure is carried out for all plasma instruments (i.e., HIA plasma beta, CODIF plasma beta, and PEACE beta versus FGM B_{xy}) separately. To ensure consistency in the IPS location between different spacecraft, the minimum value B_{xy} condition found for any of the instrument data above is used

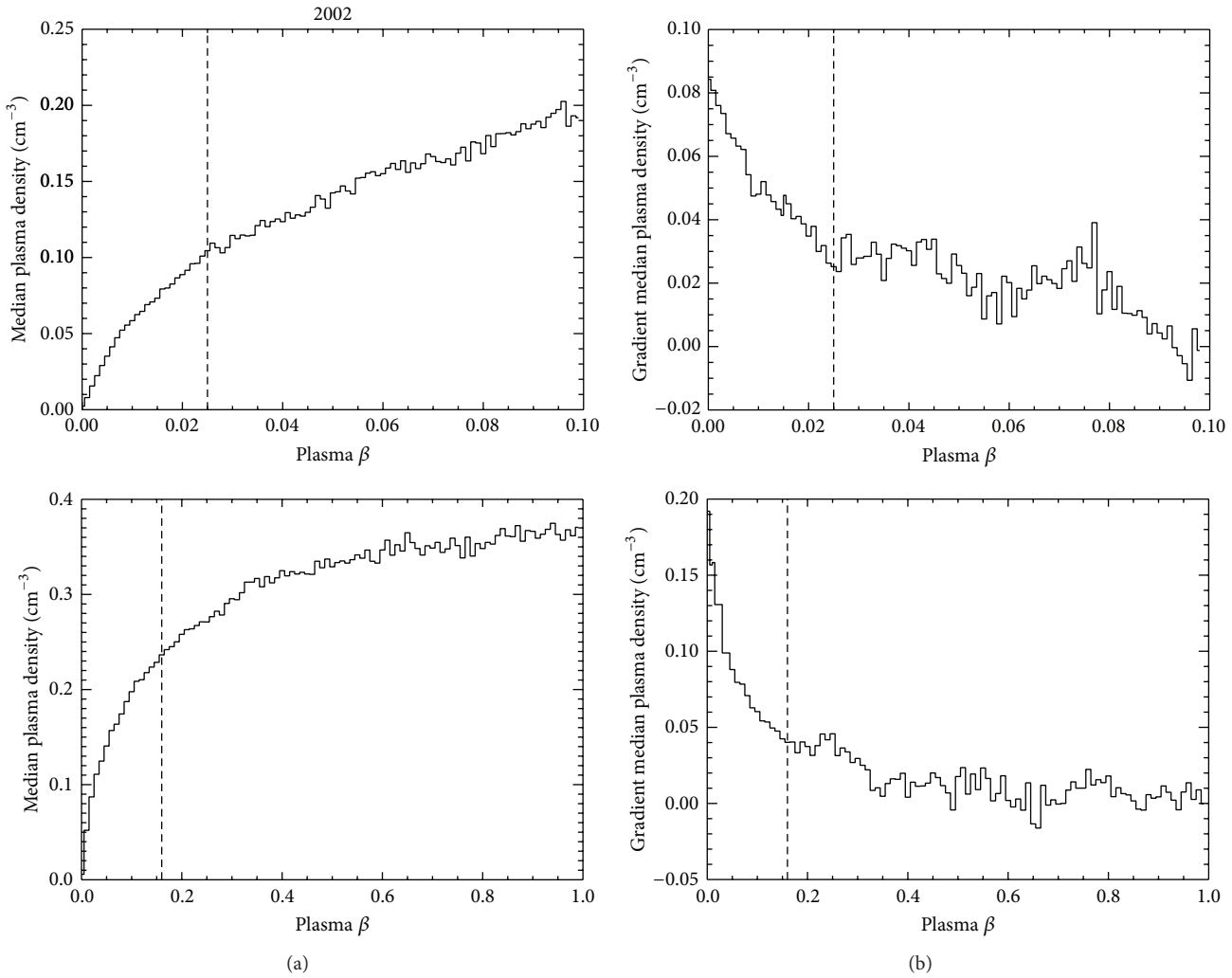

Figure 2: Histograms of Figure 1(c) data: plasma density (CODIF-H1) versus plasma beta (CODIF-H1) for the entire tail season of 2002. Left hand column: the median of binned plasma density versus beta; right hand column: the gradient of the median line. Top row beta scale shows the BR-OPS transition; bottom row shows LOBE-BR. Vertical dashed lines show the statistical BR-OPS boundary condition (top row) and the LOBE-BR boundary condition (bottom row).

Table 3: 3σ values of plasma flow velocities determined from all flow velocities recorded in plasma sheet regions during one tail season (July–October). Values are used as thresholds in determination of the percentage of high speed flow during region intervals.

Year	HIA Vpar (km s^{-1})	HIA Vperp (km s^{-1})	CODIF H1 Vpar (km s^{-1})	CODIF H1 Vperp (km s^{-1})
2001	182	141	243	164
2002	208	137	356	257
2003	185	189	274	216
2004	174	128	286	206
2005	160	126	332	257
2006	144	150	334	284
2007	132	123	368	325
2008	131	134	402	378
2009	99	95	260	240

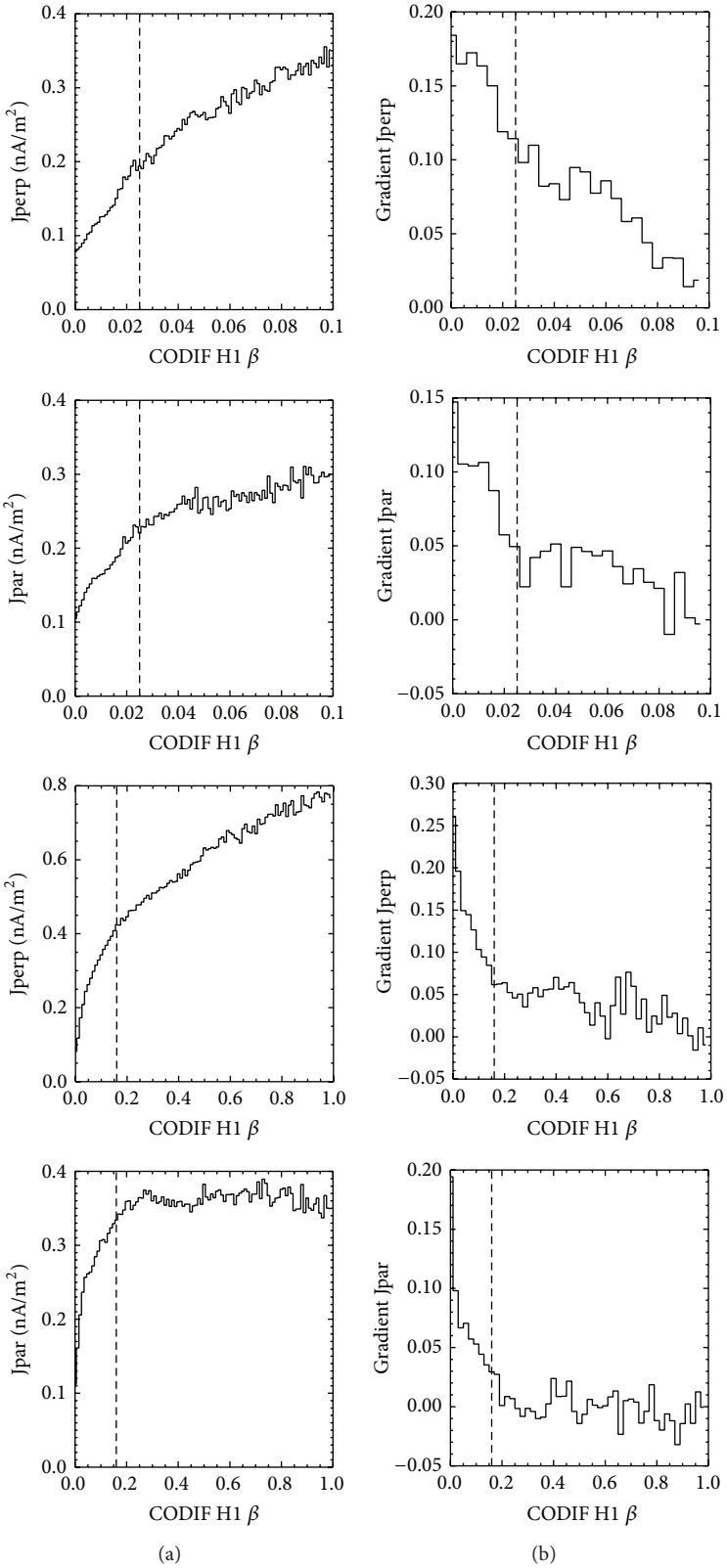

Figure 3: Histograms of data from Figures 1(a) and 1(b): perpendicular (Jperp) and parallel (Jpar) currents versus plasma beta on two scales showing the LOBE-BR transition, top two rows, and the BR-OPS transition region, bottom two rows. Left hand column is the median of binned current versus beta; the right hand column is the gradient of the median line. Dashed lines show the statistical boundaries.

Table 4: Values of electron beta used in determination of high beta OPS regions/low beta IPS regions, when the PEACE instrument is used in region identification, that is, the ratio of ion to electron beta at ion beta 1 for each tail season.

Year	High electron (PEACE) beta value
2001	0.2
2002	0.2
2003	0.25
2004	0.26
2005	0.37
2006	0.36
2007	0.43
2008	0.45
2009	0.26

as the final condition on all spacecraft for that year. Inside the IPS regions unusually low beta may exist (e.g., cold tenuous plasma near the neutral sheet after long periods of northward interplanetary magnetic field); conversely OPS regions with unusually high beta may also be of interest. Both such regions are flagged in the dataset. For regions determined using ion beta (CODIF H1 or HIA instrument used; see the following) a beta value of 1 (an important boundary where the ion pressure starts to dominate the magnetic field pressure) is used to flag low beta IPS or high beta OPS regions. If the PEACE (electrons) instrument is used, the statistical ratio found between ion and electron beta at an ion beta value of 1 for the relevant year is used to determine the equivalent value of electron beta. The electron beta values used for each year are listed in Table 4.

Finally, crossings of the neutral sheet (the centre of the plasma sheet where the B_x component of the magnetic field goes to zero such that above the boundary is northern magnetic hemisphere and below southern magnetic hemisphere) are also identified and recorded as a neutral sheet region (NSR).

(5) Neutral Sheet Region (NSR). It is the time interval of data points bracketing crossing of $B_x = 0$. We allow a NSR region to be as long as 32 seconds (consistent with the length of data gaps allowed; see the following discussion). If two consecutive data points are found in opposite hemispheres (i.e., one with $B_x > 0$; the next with $B_x < 0$, or vice versa) but are apart further than 32 seconds, an NSR region is not recorded. We record the hemisphere of the spacecraft in the region names such that in this case the crossing of the neutral sheet will be observed by two consecutive plasma regions of opposite hemispheres. Since regions are determined from maximum 4-second resolution data, and often longer, it is possible for IPS, OPS, or BR intervals to contain multiple NS crossings at the 5 Hz resolution if the spacecraft cross the neutral sheet and return to the same hemisphere within the time resolution of the input merged plasma and magnetic field moments dataset used in region determination. Therefore, the number of neutral sheet crossings ($B_x = 0$) found in the high resolution 5 Hz (200 ms) FGM CAA dataset is recorded in each region record.

For a variety of reasons which are listed in the parameter description below, plasma regions cannot be identified for all intervals within each day. These intervals are recorded as an undefined region (UR) in the dataset.

(6) Undefined Region (UR). It is the intervals where plasma regions could not be identified. There are several reasons why UR records may be needed. For example, we only identify plasma regions in the tail box region as $X < -8R_E$, $|Y| < 15R_E$. Outside of this region, the plasma environment can change drastically due to new plasma regimes being encountered in the flanks or inner magnetosphere. All intervals when the Cluster spacecraft are outside the defined tail region box are recorded with a UR record. In order to maintain as much accuracy in region identification as possible, while not increasing the number of region records to the point of a new record for every data point in the input dataset, we allow a maximum data gap of 32 seconds between the input merged plasma-magnetic field data points within one region record. That is, if two consecutive data points record the same plasma region but are separated by more than 32 seconds we consider this to be too long an interval to assume that the spacecraft have remained in the same plasma region, and we therefore split the plasma region in two, separating the regions with a UR region record spanning +3 seconds from the end of the first plasma region record to −3 seconds prior to the second time (3 seconds is 1 second greater than the half interval of the dataset resolution, i.e., 2 seconds, and therefore this prevents any overlap). The value of 32 seconds has been chosen through testing maximization of the accuracy of region identification without increasing the number of UR records to unmanageable or impractical numbers.

To avoid region identification in nontail regions, for example, magnetosheath, solar wind, mantle, and so forth, we identify tail regions only in the tail box $X < -8R_E$, $|Y| < 15R_E$ GSM. However, during extreme solar wind events (when the solar wind ram pressure impinged on the magnetosphere is great) it is possible that the spacecraft will enter these regions due to the severe compression of the magnetotail. Sheath regions will be recorded as plasma sheet by the search algorithm due to the high plasma density and beta in the magnetosheath, and such intervals have been identified in our dataset. In an attempt to remove magnetosheath entries from the database, we move all plasma regions in the flanks, $|YZ| > 10R_E$ (where $YZ = \sqrt{Y^2 + Z^2}$), which exhibit a maximum tailward flow speed of greater than 300 km s^{-1} and plasma density of greater than 1 particle/cm^3 (a clear signature of magnetosheath flow) to a UR region record. These conditions remove magnetosheath entry without removal of plasma sheet flows.

While a high tailward flow velocity identifies the majority of sheath entries, other nontail plasma regions near the magnetopause, such as the mantle boundary layer, may be entered without the observation of high speed flow. However, such regions may be identified by the extreme high plasma density recorded in these regions. Unphysical, very high density plasma may also be recorded by all three plasma instruments due to rare instrumental errors. Such regions are removed to UR if the conditions $|YZ| > 8R_E$ plasma density

> 10 particles/cm^3 or $|YZ| > 14R_E$ plasma density > 2 particles/cm^3 are met. While the conditions have been chosen, based on statistics and investigation of such intervals, to remove all nontail region plasma regimes to UR region records, it is possible that some rare nontail regions remain in the dataset in the flank regions when the density recorded is lower than the automatic removal conditions described above. Such regions are impossible to discern from the cold dense plasma sheet based on plasma and magnetic field moments alone. Regions with statistically unusually high density in the flanks are flagged ($|YZ| > 8R_E$ plasma density > 1 particle/cm^3).

While strong tailward velocity flows can be used to remove magnetosheath regions when CIS-HIA or CIS-CODIF plasma velocity is available, when only electron data from the PEACE instrument is available, as on Cluster 2, the velocity data is not accurate enough to remove such intervals. In the years 2001–2004 spacecraft separation is small such that all spacecraft are expected to observe the same plasma regions simultaneously. Therefore, for C2 we remove all plasma regions which fall within the time interval of a magnetosheath or high density UR region (as described above) identified by the C1, C3, or C4 spacecraft in the years 2001–2004. The spacecraft separation is much greater after 2004 such that C2 is not expected to be in the same plasma regions as other spacecraft at the same time, and therefore such a method cannot be used. Therefore all C2 plasma regions in the flanks ($|YZ| > 10R_E$) are flagged, and this data should be treated with caution due to possible magnetosheath/magnetopause boundary layer entry during rare events.

When spacecraft cross the magnetopause the X component of the magnetic field (B_x) can change sign such that if a spacecraft crosses from the southern hemispheric lobe to the magnetosheath, a reversal of B_x from negative to positive can be seen, and vice versa on a return crossing. This leads to an NSR identification by the region search algorithm, as $B_x = 0$ has been crossed. Obviously such crossings are not crossings of the tail neutral sheet and should be removed from the dataset. Both high density and high velocity conditions used in region removal described above are often not met during these crossings, and we therefore remove all NSR regions from the dataset to a UR record if the spacecraft Z location is greater than $5R_E$ (based on statistical results and crossing investigation). Regions removed due to high density conditions or magnetopause crossing may still be of interest to scientists and therefore the averaged characteristic region parameters for all regions removed to UR due to crossing of the magnetopause or extreme density conditions remain recorded in the region files, and the plasma region previously recorded by the search algorithm (e.g., NSR, IPS, etc.) is given by the comment flag.

Solar proton events (SEPs) are associated with coronal mass ejections (CMEs) at the Sun. Protons can be accelerated to very high energies by solar flares or interplanetary shocks associated with CMEs. These highly energetic particles can pass through the spacecraft walls and directly interfere with the plasma instruments on-board Cluster, effecting plasma region identification. Therefore, using a list of SEP events identified and made publically available, by the U.S. Department of Commerce, NOAA, Space Weather Prediction Center (http://www.swpc.noaa.gov/ftpdir/indices/SPE.txt), we remove all region identifications from the start time of every SEP event recorded in the list which has a proton flux, measured in particle flux units (pfu) integrated over a 5-minute average for energies > 10 Mev, of greater than 300, until exactly two days after the time of maximum. The NOAA list provides a start time for each event, as well as a time of maximum, but an event end time is not specified. The length of interval to remove, and significant flux level, has therefore been chosen based on visual inspection of all SEP events in the Cluster tail season. That is, it is judged that the instruments are affected for a maximum of two days past the time of maximum flux. A total of nine SEP event intervals are recorded in the tail season of 2001–2009.

A further issue arises with data quality on the Cluster 4 spacecraft after 2003. It is known that the CODIF instrument both degrades and may only partially detect the full plasma distribution after 2003 when it is in the most common operation modes, due to a reduced energy sweep range. The degradation of the instrument causes large fluctuations to be recorded in plasma moments such that region identification based on any plasma criteria threshold value is difficult; that is, regions can change every data point, especially in the low density lobe-BR intervals. For this reason, the HIA instrument is used in region identification on the C1 and C3 spacecraft after 2003. However, HIA is not operational on C4 and PEACE data is only very sporadic, leaving CODIF as the only viable option. CODIF region identification on C4 after 2003 is still useful in that visualizing the region identification indicates whether the spacecraft is in lobe, near the edge of the plasma sheet (BR identifications interspersed with many lobe identifications), deeper into the plasma sheet (rapidly changing OPS and BR regions recorded), or in the IPS (where the IPS condition is based on magnetic field data such that IPS region identification is nominal for all intervals). However, due to the large inaccuracy/variability of region identification at the lobe-BR, BR-OPS interfaces, the region identification from C4 after 2003 should not be used in blind statistics and should be used with caution.

Several validation efforts have been made to check the accuracy of the region identification. Region identifications were compared between the four spacecraft in the years 2001–2004, when the spacecraft were close together and therefore were expected to see the same plasma regions (e.g., test of consistency between region identification from the different plasma instruments used for each spacecraft). Region identification during specific dynamical magnetotail events (e.g., tail reconnection, fast flows, and wavy current sheet) was checked for consistency. Region thresholds during geomagnetic storm and nonstorm time were compared and found to be consistent. Many region boundary crossings were compared to other thresholds or boundaries determined by eye and found to be consistent or better than other methods.

For each day of the month, for each spacecraft, and for each tail season month of the Cluster mission dataset 2001–2009, the search algorithm tests the merged input datasets for the region conditions described in Table 1. An epoch ordered

list of which plasma region each spacecraft has observed, from the start to end of each day, is created where each region is described by an entry and exit time and averaged characteristic plasma and magnetic field parameters. The magnetic hemisphere ($B_x > 0$ northern hemisphere, $B_x < 0$ southern) of each region is incorporated in the region name, for neutral sheet crossing regions the direction of the crossing is given. A full list of the regions identified is given in Table 2.

3. Dataset Description

The dataset associated with this Dataset Paper consists of 2 items which are described as follows.

Dataset Item 1 (Table). ASCII file for each spacecraft (C1, C2, C3, and C4) at years 2001–2005. The file contains a continuous time series epoch ordered tabulated list of plasma regions encountered by the spacecraft covering the four tail session months (July–October) of the dataset. Each record in the file represents one plasma region encounter, with the entry and exit of the region and averaged characteristic plasma and magnetic field parameters. The parameters and their representation have been chosen through consultation with the expected user communities and are expected to fully describe the average region characteristics and activity levels needed to fully understand these plasma regimes. The Region Interval column presents the ISO time range, entry and exit time, of each plasma region, for example, 2001-10-28T00:00:00.000Z/2001-10-28T02:08:31.087Z (corresponding to a region entry time of year 2001, month 10, day 28, hour 00, minute 00, second 00, and milliseconds 000, and a region exit time of year 2001, month 10, day 28, hour 02, minute 08, second 31, and milliseconds 087). Merged CAA Cluster moments (spin resolution, 4 seconds) are used in region identification such that time tags of each plasma region are the time tags of the first Cluster magnetic field moment (FGM) meeting the region criteria and the last one meeting the criteria before region change. The first region entry time for each day of the year is of the form, for example, 2001-10-28T00:00:00.000Z, and the last region exit time of each day will be of the form, for example, 2001-10-28T23:59:59.999Z. The Region Name column represents which region has been encountered and incorporates which magnetic hemisphere the region belongs to or in the case of NSR regions the direction of the crossing. The Mean B_{xy} column represents the mean value of the FGM xy component ($B_{xy} = \sqrt{B_x^2 + B_y^2}$) of the magnetic field in the region interval. The SD of B_{xy} column represents the standard deviation of FGM B_{xy} (GSM) in the region interval. The Mean B_z column represents the mean FGM B_z (GSM) component in the region interval. The Minimum and Maximum B_z columns represent the minimum and maximum values of the B_z (GSM) component of the magnetic field in the region. The Mean Density column represents the mean value of the plasma density (electron or ion density, depending on the plasma instrument used) in the region interval. The Mean Total Pressure column represents the mean value of the total pressure in the region interval, $P = nkT + 2\mu_0 B^2$. The Median Plasma Beta column represents the median value of plasma beta (ion beta-HIA or CODIF or electron beta-PEACE, depending on the instrument used) in the region interval. The High Vpar and Vperp Percent columns represent the percentage of data points in the region interval recording high speed parallel and perpendicular flow speeds, respectively. The Minimum and Maximum Vx columns represent the minimum and maximum values of the x component of the plasma flow in the region interval. The Spacecraft X Location, Spacecraft Y Location, and Spacecraft Z Location columns, respectively, represent the X, Y, and Z locations of the spacecraft at the time of region entry, in GSM coordinates and units of Earth radii. The NS Crossings Number column indicates the number of multiple neutral sheet crossings in the interval, determined from the FGM 5 Hz (200 ms) high resolution dataset. The Number of Data Points column shows the number of data points in the region interval (nearest neighbour merged FGM and plasma moments data). The Minimum and Maximum Time Interval columns, respectively, represent the minimum and maximum time intervals between data points in the region to the nearest second. They provide information on the accuracy of region determination. If the minimum resolution of the data points within the region is large (maximum 32 seconds) then the user may wish to examine this interval more carefully. The Number of Gaps column indicates the number of times the time interval between data points in the region interval is greater than half the allowed time gap between data points before the region is split into two with a data gap (UR) region record (allowed gap = 32 seconds), giving more information on the accuracy of the region determination. If the value of n_gaps/n is large, it is recommended that the user should treat the region with caution. The UR Flag column gives the reason for a UR record (values—0: this is not a UR record; 1: missing FGM moments; 2: missing plasma moments; 3: missing both FGM and plasma moments; 4: spacecraft outside of tail region box $X < -8R_E$, $|Y| < 15R_E$; 5, 6, and 7: flag 4 + flags 1–3 (i.e., the spacecraft is outside the tail box for some period of the UR region; there are also missing FGM moments (flag 5), missing plasma moments (flag 6), or missing both FGM and plasma moments (flag 7)); 8: FGM instrument caveats found during the period; 9: plasma instrument caveats found during the period; 10: plasma and/or FGM instrument is in the wrong operation mode (e.g., calibration/test mode; see list of instrument modes in CAA instrument documentation); 11: possible magnetosheath entry; 12: region has been removed due to very high density in the flanks of the tail ($|YZ| > 8R_E$ plasma density > 10 particles/cm^3 or $|YZ| > 14R_E$ plasma density > 2 particles/cm^3); 13: NSR interval removed to UR when spacecraft $|Z| > 5$ (e.g., crossing of magnetopause into the solar wind, not a crossing of the NS); 14: C2 interval in which other spacecraft record magnetosheath entry (UR flag 11 or 12 seen by C1, C3, or C4), applied only in 2001–2004 (when the spacecraft are close); 15: solar proton event recorded in interval). The Instrument Quality Flag column describes the plasma and magnetic field instrument CAA standard quality flags for the interval (values—0: not applicable; both FGM and plasma instrument quality flags

are set to 0; 1: known problems; either FGM or plasma instrument quality flag is set to 1 (known problems) or 2 (survey data); 3: good for publication, subject to PI approval; if FGM and plasma quality flag are both set to 3 (good for publication, subject to PI approval) or 4 (excellent data); 10: flag for other known issues, always set for C4 regions after 2003, when data quality degrades). The Comment Flag column describes statistically unusual regions, and for NSR regions the plasma regions (IPS, OPS, etc.) encountered on the crossing (values—0: no comment; 1: OPS region with high beta data points (>1 for ions, ratio for electrons); 2: IPS region contains data points with low beta data points (<1 for ions, ratio for electrons); 3: IPS region with minimum beta in the statistical BR beta range; 4: IPS region with minimum beta in the lobe beta range; 5: lobe region containing data points where the plasma density measured is below the instrument threshold (i.e., CAA moments record density of 0) may result in no beta or averaged plasma parameters in region record; 6: lobe region with density typical of plasma sheet, density $>0.1\,\mathrm{cm}^{-3}$; 7: region in the flanks ($|YZ| > 8$) with unusually high density ($>1\,\mathrm{cm}^{-3}$); 8–12: records which plasma region was removed to a UR region when extreme density condition is met (UR flag condition 12). 8 = NSR, 9 = IPS, 10 = OPS, 11 = BR, and 12 = LOBE; 13: C2 region in the flanks $|YZ| > 10$; 14: C2 region in the flanks is lobe with high density ($>0.1\,\mathrm{cm}^{-3}$); 66–99: the plasma region covered by NSR regions (66: NSR region contains IPS data points only; 67: NSR region contains IPS and OPS data points; 68: NSR region contains IPS and BR data points; 69: NSR region contains IPS and LOBE data points; 77: NSR region contains OPS data points only; 78: NSR region contains OPS and BR data points; 79: NSR region contains OPS and LOBE data points; 88: NSR region contains BR data points only; 89: NSR region contains BR and LOBE data points; 99: NSR region contains LOBE data points only)). The Instrument ID column is the ID of the plasma instrument used (0: not applicable; 1: CIS-CODIF_H1; 2: CIS-HIA; 3: PEACE).

Column 1: Year
Column 2: Spacecraft Number
Column 3: Region Interval
Column 4: Region Name
Column 5: Mean B_{xy} (nT)
Column 6: SD of B_{xy} (nT)
Column 7: Mean B_z (nT)
Column 8: Minimum B_z (nT)
Column 9: Maximum B_z (nT)
Column 10: Mean Density (cm^{-3})
Column 11: Mean Total Pressure (nPa)
Column 12: Median Plasma Beta
Column 13: High Vpar Percent (%)
Column 14: High Vperp Percent (%)
Column 15: Minimum Vx ($\mathrm{km\,s}^{-1}$)
Column 16: Maximum Vx ($\mathrm{km\,s}^{-1}$)
Column 17: Spacecraft X Location (R_E)
Column 18: Spacecraft Y Location (R_E)
Column 19: Spacecraft Z Location (R_E)
Column 20: NS Crossings Number
Column 21: Number of Data Points
Column 22: Minimum Time Interval (s)
Column 23: Maximum Time Interval (s)
Column 24: Number of Gaps
Column 25: UR Flag
Column 26: Instrument Quality Flag
Column 27: Comment Flag
Column 28: Instrument ID

Dataset Item 2 (Table). ASCII file for each spacecraft (C1, C2, C3, and C4) at years 2006–2009. The file contains a continuous time series epoch ordered tabulated list of plasma regions encountered by the spacecraft covering the four tail session months (July–October) of the dataset. Each record in the file represents one plasma region encounter, with the entry and exit of the region and averaged characteristic plasma and magnetic field parameters. The parameters and their representation have been chosen through consultation with the expected user communities and are expected to fully describe the average region characteristics and activity levels needed to fully understand these plasma regimes. The Region Interval column presents the ISO time range, entry and exit time, of each plasma region, for example, 2001-10-28T00:00:00.000Z/2001-10-28T02:08:31.087Z (corresponding to a region entry time of year 2001, month 10, day 28, hour 00, minute 00, second 00, and milliseconds 000, and a region exit time of year 2001, month 10, day 28, hour 02, minute 08, second 31, and milliseconds 087). Merged CAA Cluster moments (spin resolution, 4 seconds) are used in region identification such that time tags of each plasma region are the time tags of the first Cluster magnetic field moment (FGM) meeting the region criteria and the last one meeting the criteria before region change. The first region entry time for each day of the year is of the form, for example, 2001-10-28T00:00:00.000Z, and the last region exit time of each day will be of the form, for example, 2001-10-28T23:59:59.999Z. The Region Name column represents which region has been encountered and incorporates which magnetic hemisphere the region belongs to or in the case of NSR regions the direction of the crossing. The Mean B_{xy} column represents the mean value of the FGM xy component ($B_{xy} = \sqrt{B_x^2 + B_y^2}$) of the magnetic field in the region interval. The SD of B_{xy} column represents the standard deviation of FGM B_{xy} (GSM) in the region interval. The Mean B_z column represents the mean FGM B_z (GSM) component in the region interval. The Minimum and Maximum B_z columns represent the minimum and maximum values of the B_z (GSM) component of the magnetic field in the region. The Mean Density column represents the mean value of the plasma density (electron or ion density, depending on the plasma instrument used) in the

region interval. The Mean Total Pressure column represents the mean value of the total pressure in the region interval, $P = nkT + 2\mu_0 B^2$. The Median Plasma Beta column represents the median value of plasma beta (ion beta-HIA or CODIF or electron beta-PEACE, depending on the instrument used) in the region interval. The High Vpar and Vperp Percent columns represent the percentage of data points in the region interval recording high speed parallel and perpendicular flow speeds, respectively. The Minimum and Maximum Vx columns represent the minimum and maximum values of the x component of the plasma flow in the region interval. The Spacecraft X Location, Spacecraft Y Location, and Spacecraft Z Location columns, respectively, represent the X, Y, and Z locations of the spacecraft at the time of region entry, in GSM coordinates and units of Earth radii. The NS Crossings Number column indicates the number of multiple neutral sheet crossings in the interval, determined from the FGM 5 Hz (200 ms) high resolution dataset. The Number of Data Points column shows the number of data points in the region interval (nearest neighbour merged FGM and plasma moments data). The Minimum and Maximum Time Interval columns, respectively, represent the minimum and maximum time intervals between data points in the region to the nearest second. They provide information on the accuracy of region determination. If the minimum resolution of the data points within the region is large (maximum 32 seconds) then the user may wish to examine this interval more carefully. The Number of Gaps column indicates the number of times the time interval between data points in the region interval is greater than half the allowed time gap between data points before the region is split into two with a data gap (UR) region record (allowed gap = 32 seconds), giving more information on the accuracy of the region determination. If the value of n_gaps/n is large, it is recommended that the user should treat the region with caution. The UR Flag column gives the reason for a UR record (values—0: this is not a UR record; 1: missing FGM moments; 2: missing plasma moments; 3: missing both FGM and plasma moments; 4: spacecraft outside of tail region box $X < -8R_E$, $|Y| < 15R_E$; 5, 6, and 7: flag 4 + flags 1–3 (i.e., the spacecraft is outside the tail box for some period of the UR region; there are also missing FGM moments (flag 5), missing plasma moments (flag 6), or missing both FGM and plasma moments (flag 7)); 8: FGM instrument caveats found during the period; 9: plasma instrument caveats found during the period; 10: plasma and/or FGM instrument is in the wrong operation mode (e.g., calibration/test mode; see list of instrument modes in CAA instrument documentation); 11: possible magnetosheath entry; 12: region has been removed due to very high density in the flanks of the tail ($|YZ| > 8R_E$ plasma density > 10 particles/cm^3 or $|YZ| > 14R_E$ plasma density > 2 particles/cm^3); 13: NSR interval removed to UR when spacecraft $|Z| > 5$ (e.g., crossing of magnetopause into the solar wind, not a crossing of the NS); 14: C2 interval in which other spacecraft record magnetosheath entry (UR flag 11 or 12 seen by C1, C3, or C4), applied only in 2001–2004 (when the spacecraft are close); 15: solar proton event recorded in interval). The Instrument Quality Flag column describes the plasma and magnetic field instrument CAA standard quality flags for the interval (values—0: not applicable; both FGM and plasma instrument quality flags are set to 0; 1: known problems; either FGM or plasma instrument quality flag is set to 1 (known problems) or 2 (survey data); 3: good for publication, subject to PI approval; if FGM and plasma quality flag are both set to 3 (good for publication, subject to PI approval) or 4 (excellent data); 10: flag for other known issues, always set for C4 regions after 2003, when data quality degrades). The Comment Flag column describes statistically unusual regions, and for NSR regions the plasma regions (IPS, OPS, etc.) encountered on the crossing (values—0: no comment; 1: OPS region with high beta data points (>1 for ions, ratio for electrons); 2: IPS region contains data points with low beta data points (<1 for ions, ratio for electrons); 3: IPS region with minimum beta in the statistical BR beta range; 4: IPS region with minimum beta in the lobe beta range; 5: lobe region containing data points where the plasma density measured is below the instrument threshold (i.e., CAA moments record density of 0) may result in no beta or averaged plasma parameters in region record; 6: lobe region with density typical of plasma sheet, density >0.1 cm^{-3}; 7: region in the flanks ($|YZ| > 8$) with unusually high density (>1 cm^{-3}); 8–12: records which plasma region was removed to a UR region when extreme density condition is met (UR flag condition 12). 8 = NSR, 9 = IPS, 10 = OPS, 11 = BR, and 12 = LOBE; 13: C2 region in the flanks $|YZ| > 10$; 14: C2 region in the flanks is lobe with high density (>0.1 cm^{-3}); 66–99: the plasma region covered by NSR regions (66: NSR region contains IPS data points only; 67: NSR region contains IPS and OPS data points; 68: NSR region contains IPS and BR data points; 69: NSR region contains IPS and LOBE data points; 77: NSR region contains OPS data points only; 78: NSR region contains OPS and BR data points; 79: NSR region contains OPS and LOBE data points; 88: NSR region contains BR data points only; 89: NSR region contains BR and LOBE data points; 99: NSR region contains LOBE data points only)). The Instrument ID column is the ID of the plasma instrument used (0: not applicable; 1: CIS-CODIF_H1; 2: CIS-HIA; 3: PEACE).

Column 1: Year
Column 2: Spacecraft Number
Column 3: Region Interval
Column 4: Region Name
Column 5: Mean B_{xy} (nT)
Column 6: SD of B_{xy} (nT)
Column 7: Mean B_z (nT)
Column 8: Minimum B_z (nT)
Column 9: Maximum B_z (nT)
Column 10: Mean Density (cm^{-3})
Column 11: Mean Total Pressure (nPa)
Column 12: Median Plasma Beta
Column 13: High Vpar Percent (%)
Column 14: High Vperp Percent (%)
Column 15: Minimum Vx (km s^{-1})
Column 16: Maximum Vx (km s^{-1})

Column 17: Spacecraft X Location (R_E)
Column 18: Spacecraft Y Location (R_E)
Column 19: Spacecraft Z Location (R_E)
Column 20: NS Crossings Number
Column 21: Number of Data Points
Column 22: Minimum Time Interval (s)
Column 23: Maximum Time Interval (s)
Column 24: Number of Gaps
Column 25: UR Flag
Column 26: Instrument Quality Flag
Column 27: Comment Flag
Column 28: Instrument ID

4. Concluding Remarks

The ECLAT dataset of magnetotail plasma regions provides an excellent new tool to facilitate the use of the wealth of Cluster spacecraft data for all scientists. The dataset can be employed to gain new and important knowledge of the magnetotail plasma sheet regions and processes occurring therein and to facilitate coordinated research between solar wind, magnetospheric, and ionospheric research and scientists.

Dataset Availability

The dataset associated with this Dataset Paper is dedicated to the public domain using the CC0 waiver and is available at http://dx.doi.org/10.1155/2014/684305/dataset. In addition, the data are available in the database under "Magnetotail regions" at http://www.iwf.oeaw.ac.at/eclat/.

Conflict of Interests

The authors declare that there is no conflict of interests regarding the publication of this paper.

Acknowledgments

The authors acknowledge the European Union Framework 7 Programme, the ECLAT Project FP7 Grant no. 263325, and the ESA Cluster Active Archive in any publications based upon the use of these data. The authors would like to thank the many dedicated scientists and instrument teams that have made the Cluster mission possible. They thank Elena Grigorenko for useful discussions and provision of boundary crossings determined from velocity distributions. Thanks are also due to Alexandra Alexandrova, Martina Edl, and Daniel Schmid for testing of the dataset.

References

[1] J. W. Dungey, "Interplanetary magnetic field and the auroral zones," *Physical Review Letters*, vol. 6, no. 2, pp. 47–48, 1961.

[2] W. Baumjohann, G. Paschmann, N. Sckopke, C. A. Cattell, and C. W. Carlson, "Average ion moments in the plasma sheet boundary layer," *Journal of Geophysical Research A: Space Physics*, vol. 93, no. 10, pp. 11507–11520, 1988.

[3] V. Angelopoulos, C. F. Kennel, F. V. Coroniti et al., "Statistical characteristics of bursty bulk flow events," *Journal of Geophysical Research A: Space Physics*, vol. 99, no. 11, pp. 21257–21280, 1994.

[4] A. Åsnes, R. W. H. Friedel, B. Lavraud, G. D. Reeves, M. G. G. T. Taylor, and P. Daly, "Statistical properties of tail plasma sheet electrons above 40 keV," *Journal of Geophysical Research A: Space Physics*, vol. 113, no. 3, 2008.

[5] A. Raj, T. Phan, R. P. Lin, and V. Angelopoulos, "Wind survey of high-speed bulk flows and field-aligned beams in the near-Earth plasma sheet," *Journal of Geophysical Research A: Space Physics*, vol. 107, no. 12, pp. SMP 3-1–SMP 317, 2002.

[6] A. P. Walsh, C. J. Owen, A. N. Fazakerley, C. Forsyth, and I. Dandouras, "Average magnetotail electron and proton pitch angle distributions from Cluster PEACE and CIS observations," *Geophysical Research Letters*, vol. 38, no. 6, 2011.

[7] E. E. Grigorenko, R. Koleva, and J. A. Sauvaud, "On the problem of Plasma Sheet Boundary Layer identification from plasma moments in Earth's magnetotail," *Annales Geophysicae*, vol. 30, no. 9, pp. 1331–1343, 2012.

[8] E. Grigorenko and R. Koleva, "Variability of discrete plasma structures in the lobe-plasma sheet interface," *Comptes Rendus de L'Academie Bulgare des Sciences*, vol. 62, no. 11, pp. 1449–1454, 2009.

[9] C. P. Escoubet, M. Fehringer, and M. Goldstein, "The cluster mission—introduction," *Annales Geophysicae*, vol. 19, no. 10–12, pp. 1197–1200, 2001.

[10] T. Terasawa, M. Fujimoto, T. Mukai et al., "Solar wind control of density and temperature in the near-Earth plasma sheet: WIND/GEOTAIL collaboration," *Geophysical Research Letters*, vol. 24, no. 8, pp. 935–938, 1997.

[11] H. Laakso, M. Taylor, and C. P. Escoubet, *The Cluster Active Archive*, Springer, Amsterdam, The Netherlands, 2010.

[12] A. Balogh, C. M. Carr, M. H. Acuña et al., "The cluster magnetic field investigation: overview of in-flight performance and initial results," *Annales Geophysicae*, vol. 19, no. 10–12, pp. 1207–1217, 2001.

[13] H. Rème, C. Aoustin, J. M. Bosqued et al., "First multispacecraft ion measurements in and near the Earth's magnetosphere with the identical Cluster ion spectrometry (CIS) experiment," *Annales Geophysicae*, vol. 19, no. 10–12, pp. 1303–1354, 2001.

[14] A. D. Johnstone, C. Alsop, S. Burge et al., "Peace: a plasma electron and current experiment," *Space Science Reviews*, vol. 79, no. 1-2, pp. 351–398, 1997.

[15] M. W. Dunlop, A. Balogh, K. H. Glassmeier, and P. Robert, "Four-point Cluster application of magnetic field analysis tools: the Curlometer," *Journal of Geophysical Research A: Space Physics*, vol. 107, no. 11, pp. SMP 23-1–SMP 2314, 2002.